Semicond. Sci. Technol. 9 (1994) 811–814. Printed in the UK

The electron mobility transition in n-GaAs heavily doped channels

Y Ohkura, H Mizuta, I Ohbu, O Kagaya, K Katayama and S Ihara
Central Research Laboratory, Hitachi Ltd, Kokubunji, Tokyo 185, Japan

Abstract. Low-field electron transport properties in heavily doped n-GaAs channels at 300 K are investigated by Monte Carlo simulation. The matrix element for electron–impurity scattering is obtained from the Fourier-transformed Coulomb potential accounting for the screening effects of the two-dimensional electron gas. The effects of the screening and the impurity profile are analysed. Electron mobility is calculated for several values of sheet electron density and n-GaAs thickness. For low sheet electron density, the calculated mobility increases with the sheet electron density and is almost independent of n-GaAs thickness. For high sheet electron density, the mobility approaches a constant value and becomes independent of sheet electron density. These findings are explained for the first time as a transition from a two- to three-dimensional nature and are well confirmed by our experiments.

1. Introduction

n-GaAs heavily doped channel FETS [1] show superior current drive capability and higher breakdown voltage, especially in short-channel devices, because the gate injection current is lower than in conventional HEMTS. Since the doping density increases with the reduction in device size, it is crucial to understand the electron–impurity interaction and to predict the transport properties. However, to our best knowledge this effect has not been investigated fully for heavily doped channels.

In the present work, low-field transport properties in heavily doped n-GaAs channels are investigated by Monte Carlo simulation where a parabolic band model and screened ionized-impurity interaction [2, 3] for the two-dimensional electron gas (2DEG) were used. A transition from a two- to three-dimensional nature is studied by simulation as well as experiment.

2. The electron density profiles

Before performing the Monte Carlo simulation, the electronic states of the six lowest subbands at 300 K are calculated first by solving Poisson and Schrödinger equations self-consistently for a heavily-doped n-GaAs channel heterostructure (see table 1) [2]. The wavefunction parallel to the heterointerface is assumed to be a plane wave. We account for size quantization effects only in the Γ valley as we treat only low-field mobility. Since the $Al_xGa_{1-x}As$ layer under the Schottky gate is depleted in this work, we neglect the penetration of the wavefunction of electrons in $Al_xGa_{1-x}As$ region, and assume the heterointerface to be abrupt. The results of the electron density profiles for n-GaAs thickness $d = 15$, 25 and 35 nm (see table 1) are shown in figure 1 for various values of sheet electron density n_s. On the p-GaAs side, carriers are depleted and the electron density profiles are not sensitive to n_s or the position of the heterointerface ($z = -d$). On the gate side, the profile is affected by d. However, as long as the $Al_xGa_{1-x}As$ region is depleted at relatively low n_s, the electron profile is almost independent of n-GaAs thickness. As n_s is increased by applying a higher gate bias, a nearly charge-neutral region develops and extends toward the interface. As a result, the subband separation is reduced, and the nature of the electronic states in the channel is expected to be close to those in bulk material (three-dimensional). The minimum subband separation was found to be 54 mV for $n_s = 1 \times 10^{12}\ cm^{-2}$ and 23 mV for $n_s = 7 \times 10^{12}\ cm^{-2}$. Note that this transition from two- to three-dimensional states does not occur, for example, in an inversion layer of an Si-MOSFET or HEMT, where electrons are always localized, keeping a two-dimensional nature irrespective of n_s. We will comment on the effect of this transition on electron mobility in section 4.

Table 1. Assumed parameters for i-$Al_xGa_{1-x}As$/n-GaAs/p-GaAs structure (grown on a semi-insulating GaAs substrate).

Layer	Material	Impurity concentration (cm^{-3})	Thickness (nm)
I	$Al_{0.3}Ga_{0.7}As$	Undoped	10
II	n-GaAs	N_D 3×10^{18}	15/25/35
III	p-GaAs	N_A 3×10^{16}	300

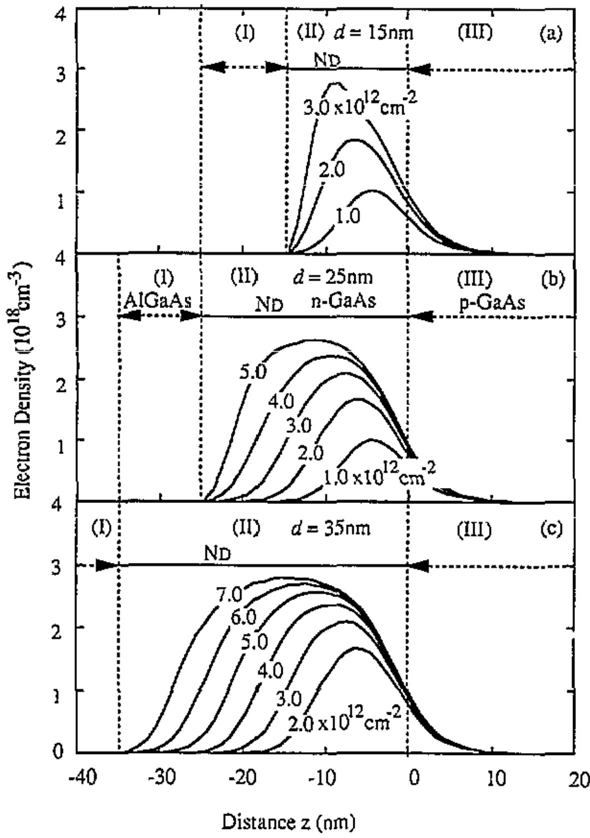

Figure 1. Calculated electron distribution for n-GaAs thickness d (a) 15 nm, (b) 25 nm, and (c) 35 nm for various values of sheet electron density. The impurity concentration in the n-GaAs ($3 \times 10^{18}\ \mathrm{cm^{-3}}$) is also shown as N_D.

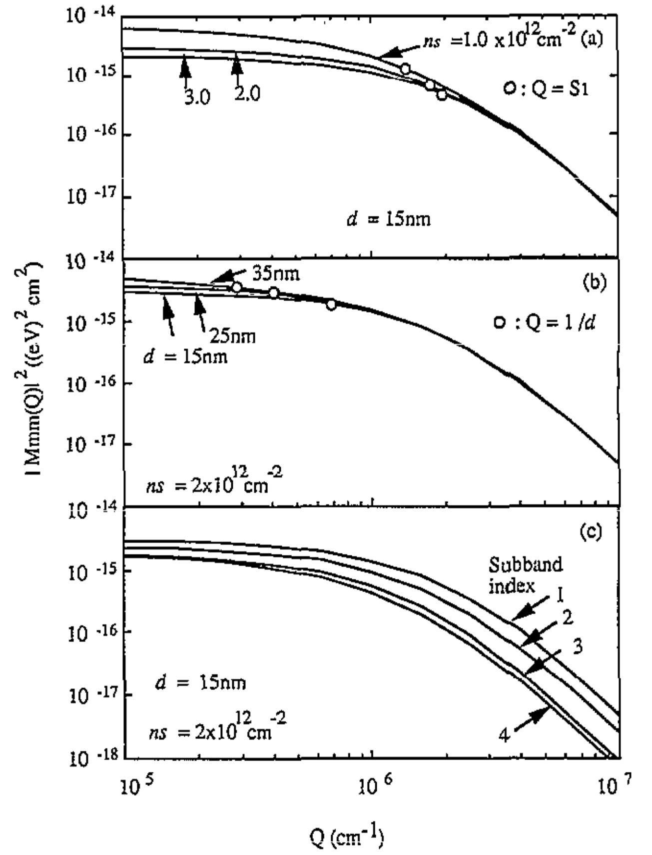

Figure 2. Calculated square of intrasubband matrix elements $|M_{mm}(Q)|^2$ for (a) different values of sheet electron density n_s with n-GaAs thickness $d = 15$ nm and $m = 1$, (b) three different n-GaAs thicknesses at $n_s = 2 \times 10^{12}\ \mathrm{cm^{-2}}$ and $m = 1$, and (c) the first four subbands with $d = 15$ nm and $n_s = 2 \times 10^{12}\ \mathrm{cm^{-2}}$. Circles indicate $Q = S_1$ (the screening constant of the first subband) in (a) and $Q = 1/d$ (n-GaAs thickness) in (b).

3. Electron–impurity interaction

Screened ionized impurity scattering for the two-dimensional electron gas (2DEG), which is used in the Monte Carlo simulations, was calculated by the approach originally proposed for MOSFETS [3]. The matrix element $M_{mn}(Q)$ is calculated from the Fourier-transformed Coulomb potential $\phi(Q, z)$ accounting for the screening effects of the 2DEG [2, 3]; here m and n are subband indices and $Q = |k_2 - k_1|$ and k_1 and k_2 are initial and final wavevectors, respectively, parallel to the layer interface. The calculated square of the intrasubband matrix element $|M_{mm}(Q)|^2$ versus Q is shown in figure 2 with (a) two-dimensional electron density n_s, (b) n-GaAs thickness d and (c) subband index as parameters. The potential $\phi(Q, z)$ induced by an impurity on located at z_0 decays approximately as $\exp(-Q|z_0 - z|)$ [2]. In other words, only the impurities within a distance $1/Q$ contribute to the scattering. The screening by electrons affects $|M_{mm}(Q)|^2$ as follows. For small Q, $\phi(Q, z)$ is slowly varying, and $|M_{mm}(Q)|^2$ corresponds to the weak scattering by impurities in a wide range. Thus the screening effect is very large. For large Q, $\phi(Q, z)$ is confined to a small region and therefore, $|M_{mm}(Q)|^2$ corresponds to strong scattering by the impurities in a very small distance and the screening effect is small.

As shown in figure 2(a), with an increase in n_s, $|M_{11}(Q)|^2$ decreases for small Q due to the screening effect. The screening constant of the first subband (S_1) [2, 3] for the three n_s values is 1.39, 1.79 and $1.95 \times 10^6\ \mathrm{cm^{-1}}$ respectively. For $Q < S_1$, the screening effect is dominant.

The dependence of $|M_{11}(Q)|^2$ on the n-GaAs thickness for $n_s = 2 \times 10^{12}\ \mathrm{cm^{-2}}$ is shown in figure 2(b). Circles in the figure indicate the points $Q = 1/d$. For Q smaller than $1/d$, $\phi(Q, z)$ decays slowly. Thus, it is clear that the n-GaAs thickness has a significant effect on $|M_{mm}(Q)|^2$.

Finally in figure 2(c), intrasubband matrix elements $|M_{mm}(Q)|^2$ versus Q are shown for the first four subbands. In the present structure, $|M_{mm}(Q)|^2$ becomes smaller for the higher subbands, as the wavefunction of higher subbands extends over the low-doped p-GaAs region. For large Q, the profile of the wavefunctions greatly affects $|M_{mm}(Q)|^2$. The subband dependence is decreased with a decrease in Q, as impurities in a wider area contribute to the scattering. This variation of $|M_{mm}(Q)|^2$ is found to be entirely different from that seen for HEMTS [2]; in HEMTS the donor ions are spatially separated from the 2DEG and the scattering is mainly due to the acceptor

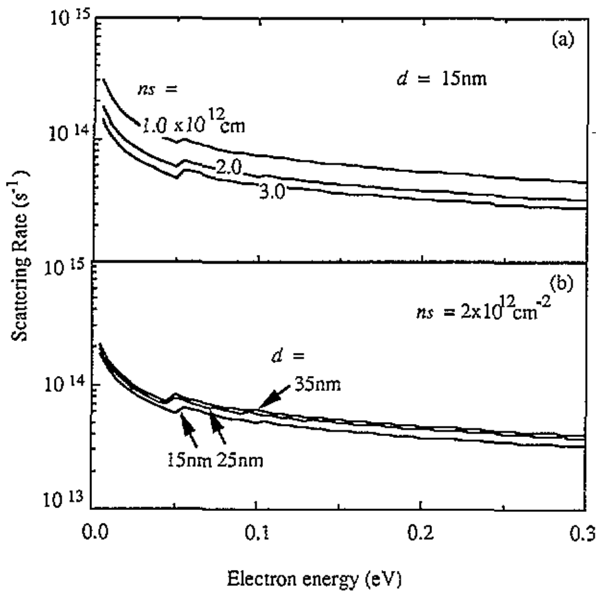

Figure 3. Ionized impurity scattering rates for the lowest subband for (*a*) different values of n_s at $d = 15$ nm and $m = 1$, (*b*) different values of d at $n_s = 2 \times 10^{12}$ cm^{-2}. The energies are measured from the bottom of the lowest subband.

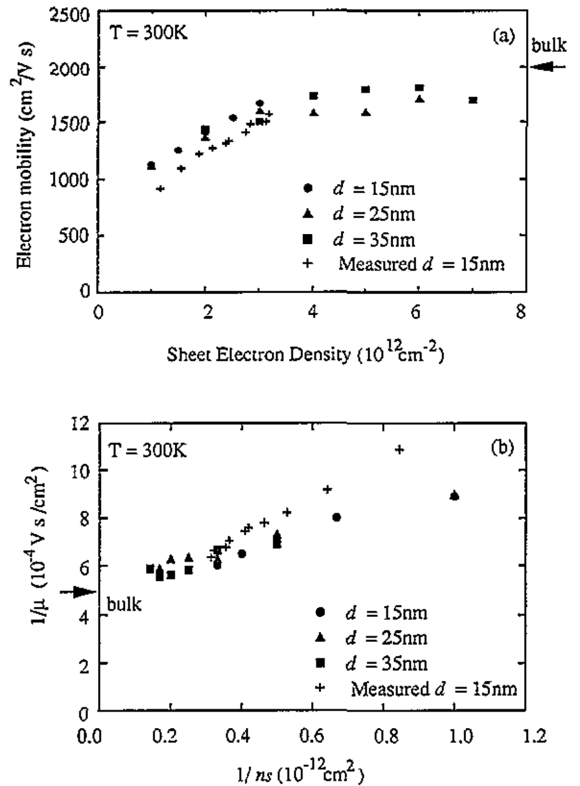

Figure 4. (*a*) Calculated electron mobility versus sheet electron density for three values of n-GaAs thickness. The measured Hall mobility for $d = 15$ nm is also shown. For comparison, the measured bulk mobility for $N_D = 3 \times 10^{18}$ cm^{-3} is shown by the arrow on the right-hand mobility axis. (*b*) Data in (*a*) shown as a $1/\mu$ versus $1/n_s$ plot.

ions in the channel. For a higher subband index, the wavefunction extends to the region of weak screening, and thus $|M_{mm}(Q)|^2$ is larger for higher subbands.

Impurity scattering rates for the first subband including intersubband transition calculated from the matrix elements are shown in figure 3 for different values of (*a*) two-dimensional electron density n_s, (*b*) n-GaAs thickness d. The dependence on n_s and d is observed for all energy values. These are due to the screening effect of the electrons and the impurity profiles respectively, as discussed previously.

In the high-n_s regime, the electrons are degenerate and the subband separation is small, so the matrix value for the intrasubband transition decreases while that for the intersubband transition increases. The total scattering rates are found to be only weakly dependent on n_s.

4. Results for low-field transport

We first describe the Monte Carlo model used for the mobility calculation. A parabolic band approximation is used and the six lowest subbands in the Γ valley of GaAs are considered. Material parameters are taken from [4]. In addition to ionized impurities, scattering rates are also calculated for polar optical, acoustic and optical phonons, following [2, 5] and including both intra- and intersubband transitions. Calculated scattering rates for phonons are not very sensitive to n_s and d, and below 10^{13} s^{-1} much less than those for impurity scattering for the present structure. A constant electric field 1 kV cm^{-1} is applied in the calculation. For this field, the average electron temperature was found to be below 400 K, so the electron density profile will not significantly deviate from the equilibrium profile. Similarly, real-space electron transfer to the AlGaAs layer and transfer to higher (L, X) valleys are negligible. Therefore, we treat the electron density profile and the screening as constant during the simulation. The degeneracy effects are included using an approximated distribution function [6] in which the Fermi energy is assumed to be the equilibrium value in section 2. An ensemble of 1000 particles is simulated for 20 ps with a constant time step (0.5 fs) discretization scheme.

The calculated low-field electron mobility (μ) is shown in figure 4(*a*). Statistical fluctuations of the results are about 100 (cm^2 V^{-1} s^{-1}). We found that the mobility increases significantly with n_s. For low n_s, the mobility is almost independent of d. This is due to the screening effect. The variation with respect to d is small when $1/d < S_1$. The mobility is found to have a simple dependence on n_s, namely, $1/\mu \simeq \alpha/n_s + \beta$, where α and β are constants (see figure 4(*b*)). In inversion layers, for low n_s, it has been shown that this dependence arises from the two-dimensional nature of electrons [3].

On the contrary, for high n_s and large d, the linearity is broken and the mobility approaches a constant value independent of n_s due to the strong screening effect, as long as the channel is nearly charge-neutral. As we

observed in section 2, for a large value of n_s, a bulk-like charge-neutral region appears in the n-GaAs channel. Therefore, the constant mobility mentioned above can be expected to be close to the three-dimensional value. Note that the three-dimensional mobility in this work is the bulk value (d is very large) and n_s is less than the doped impurity density so AlGaAs is depleted. For the very high n_s regime, the electron mobility will decrease due to real-space electron transfer to AlGaAs. The decrease in mobility has been studied extensively in the past [7]. However, here we restrict our attention to the case where there is no significant real-space transfer.

To compare with the results of the simulation, a heavily doped channel structure is fabricated by epitaxial growth with $d = 15$ nm, $N_D = 3 \times 10^{18}\ \mathrm{cm}^{-3}$ for the n-GaAs (the first case in table 1). The details of the fabrication process will be published elsewhere. The n_s dependence of Hall electron mobility has been measured at 300 K (see figure 4), for various thicknesses of the undoped top GaAs layer grown on an i-AlGaAs layer. Bulk mobility at 300 K is also measured and shown in the figure.

The low-n_s properties are in good agreement with experiments. As n_s is increased the subband separation is reduced and we expect the electron behaviour to be closer to bulk. The calculated mobility in the high-n_s regime is in fairly good agreement with the measured bulk mobility, as expected. Thus we have clearly shown, both theoretically and experimentally, that as n_s increases there is a transition in the mobility from the two-dimensional to the bulk value.

The calculated mobility is about 10–20% larger than the measured one. The probable reason for this discrepancy is that we ignored non-parabolicity and many-body effects. The latter problem has been treated in the past for the bulk case [8, 9]. However, it has not been satisfactorily resolved in the 2DEG case.

We also calculated the channel electron mobility with bulk model [5] using a two-dimensional (in real space) ensemble Monte Carlo simulator, in which the screening effect was treated using the Brooks–Herring approach [10]. The results show the n_s dependence due to the screening effect. However, as the screening in this approach is defined from 'local' electron density, the remote impurity interaction is underestimated in addition to the many-body effect [8, 9]. We found that the calculated mobility using this model is 1.5 to 2 times larger than that shown in figure 4, and that the dependence on n_s is weaker.

5. Conclusion

Low-field electron transport properties in heavily-doped n-GaAs channels at 300 K were investigated by Monte Carlo simulation. The electron–impurity interaction was obtained from the Fourier-transformed Coulomb potential accounting for the screening effects of the two-dimensional electron gas. The effects of the screening and the impurity profile were discussed. In addition, the subband dependence of impurity scattering matrix elements was found to be different from that for HEMTs. For low sheet electron density, mobility increases with the sheet electron density and is almost independent of the n-GaAs thickness. For high sheet electron density, the mobility approaches the bulk (three-dimensional) value independently of electron density. These findings were explained for the first time as a transition from two- to three-dimensional nature and are well confirmed by our experiments.

Acknowledgments

We would like to thank Drs M B Patil and Y Okuyama and T Toyabe for many useful discussions.

References

[1] Hida H *et al* 1986 *IEDM Tech. Dig.* 759
[2] Yokoyama K and Hess K 1986 *Phys. Rev.* B **33** 5595
[3] Stern F and Howard W E 1967 *Phys. Rev.* **163** 816
[4] Adachi S 1985 *J. Appl. Phys.* **58** R1
[5] Jacoboni C and Reggiani L 1983 *Rev. Mod. Phys.* **55** 645
[6] Fischetti M V and Laux S E 1988 *Phys. Rev.* B **38** 9721
[7] Littlejohn M A *et al* 1980 *J. Appl. Phys.* **51** 5445
[8] Ferry D K *et al* 1991 *Comput. Phys. Commun.* **67** 119
[9] Moore E J 1967 *Phys. Rev.* **160** 618
[10] Brooks H and Herring C 1951 *Phys. Rev.* **83** 879